



Cite this: *Environ. Sci.: Processes Impacts*, 2020, 22, 1888

## The importance of aromaticity to describe the interactions of organic matter with carbonaceous materials depends on molecular weight and sorbent geometry†

Stephanie Castan,<sup>a</sup> Gabriel Sigmund,<sup>a</sup> Thorsten Hüffer,<sup>a</sup> Nathalie Tepe,<sup>a</sup> Frank von der Kammer,<sup>a</sup> Benny Chefetz<sup>b</sup> and Thilo Hofmann<sup>\*a</sup>

Dissolved organic matter (DOM) is ubiquitous in aquatic environments where it interacts with a variety of particles including carbonaceous materials (CMs). The complexity of both DOM and the CMs makes DOM–CM interactions difficult to predict. In this study we have identified the preferential sorption of specific DOM fractions as being dependent on their aromaticity and molecular weight, as well as on the surface properties of the CMs. This was achieved by conducting sorption batch experiments with three types of DOM (humic acid, Suwannee River natural organic matter, and a compost extract) and three types of CMs (graphite, carbon nanotubes, and biochar) with different geometries and surface complexities. The non-adsorbed DOM fraction was analyzed by size exclusion chromatography and preferentially sorbed molecular weight fractions were analyzed by UV/vis and fluorescence spectroscopy. All three sorbent types were found to preferentially sorb aromatic DOM fractions, but DOM fractionation depended on the particular combination of sorbent and sorbate characteristics. Single-walled carbon nanotubes only sorbed the smaller molecular weight fractions (<1 kDa). The sorption of smaller DOM fractions was not accompanied by a preference for less aromatic compounds, contrary to what was suggested in previous studies. While graphite preferentially sorbed the most aromatic DOM fraction (1–3 kDa), the structural heterogeneity of biochar resulted in reduced selectivity, sorbing all DOM > 1 kDa. The results explain the lack of correlation found in previous studies between the amount of aromatic carbon in a bulk DOM and its sorption coefficient. DOM sorption by CMs was generally controlled by DOM aromaticity but complex sorbent surfaces with high porosity, curvatures and functional groups strongly reduced the importance of aromaticity.

Received 17th June 2020  
Accepted 9th August 2020

DOI: 10.1039/d0em00267d

rsc.li/epsi

### Environmental significance

Dissolved organic matter (DOM) is ubiquitous in surface waters, playing a major role in the global carbon cycle. Similarly, carbonaceous materials (CMs) are released in large quantities amounting to Tg per year into environmental systems, where they can play a considerable role as sorbents of DOM. Their interactions can affect the fate of both DOM and CMs. We investigated preferentially sorbing DOM fractions in dependence of their aromaticity and molecular weight as well as the CM surface properties using a range of different DOM and CM types. The influence of sorbate and sorbent properties on the interactions were shown to be strongly interdependent. The results improve a mechanistic understanding of the factors influencing sorption of DOM to CMs.

## 1. Introduction

Natural organic matter (NOM) derived from decaying plant and microbial biomass is ubiquitous in the natural environment,

playing a major role in the global carbon cycle.<sup>1</sup> In general, for a water sample, a filter cutoff between 0.2 and 0.7  $\mu\text{m}$  is used operationally to define the dissolved organic matter (DOM) fraction of NOM.<sup>2</sup> It comprises a complex mixture of humic substances, carbohydrates, lipids, proteins, and other bio-macromolecules, that cover a continuum of molecular weights ranging from a few hundred Dalton (Da) to >100 000 Da.<sup>3</sup> DOM aromaticity and the presence of functional groups depends on its origin.<sup>4</sup> Of this variety of compounds, operationally defined humic acid (HA) and fulvic acid (FA) have often been used as surrogate compounds to represent DOM in experiments.<sup>5</sup> Because of its ubiquitous distribution, DOM can influence the

<sup>a</sup>Environmental Geosciences, Centre for Microbiology and Environmental Systems Science, University of Vienna, Althanstraße, 1090 Wien, Austria. E-mail: thilo.hofmann@univie.ac.at

<sup>b</sup>Department of Soil and Water Sciences, Faculty of Agriculture, Food and Environment, The Hebrew University of Jerusalem, P.O. Box 12, Rehovot 7610001, Israel

† Electronic supplementary information (ESI) available. See DOI: 10.1039/d0em00267d



surface charge, aggregation, and transport of particles, including carbonaceous material (CM) particles, that are present in natural environments.<sup>6</sup>

CMs can be produced as a result of incomplete biomass combustion or pyrolysis, as well as petrogenic processes, and are released as particles into the environment in large quantities, amounting to several Tg of carbon per year.<sup>7</sup> CMs such as biochar or activated carbon can be deliberately introduced into the environment for contaminant remediation, soil improvement, or carbon mitigation. On the other hand, carbon nanotubes, fullerenes, and graphite used for technological applications can enter the environment unintentionally during any stage of their life cycles.<sup>7,8</sup> Naturally produced CMs such as soot or wildfire chars constitute the largest pool of CMs in the natural environment and can play a considerable role in environmental systems. Once introduced into surface waters, the high sorption capacity of CMs make them effective sorbents for DOM in aqueous systems, affecting the fate of both the DOM and the CMs.<sup>5</sup>

Understanding the interactions between DOM and CMs is rendered difficult by the complexity and heterogeneity of DOM. Sorption is often driven by  $\pi$ - $\pi$  electron-donor-acceptor (EDA) interactions. Other sorption mechanisms include H-bonds, electrostatic interactions, and hydrophobic effects, with their relative contributions to overall sorption depending on the properties of both sorbent and sorbate.<sup>9,10</sup> Sorbent properties, such as the diameters of carbon nanotubes or the presence of surface functional groups, can affect sorption.<sup>9,11-13</sup> Furthermore, the different chemical and size fractions of DOM are not sorbed equally. Smaller DOM molecules can sorb in mesopores of CMs, while bigger molecules are excluded through steric hindrance,<sup>14-16</sup> but generally preferential sorption of aromatic and high molecular weight DOM fractions by CMs was observed.<sup>9,10,14,17,18</sup> Hence, the percentage of aromatic carbon in a bulk DOM sample would be expected to relate to the extent of sorption to CMs. However, a recently published review on the sorption of a large variety of DOM to carbon nanotubes found no such correlation.<sup>5</sup> Further investigation of the factors other than aromaticity that affect sorption was therefore required to explain this discrepancy.

Since each molecular weight fraction of DOM exhibits different chemical properties, adsorptive fractionation should be regarded as a combined effect of both chemical and physical characteristics. In this study we have therefore analyzed the effect of DOM aromaticity, molecular weight, and CM surface properties on DOM sorptive fractionation. For this purpose, different DOM types of increasing complexity regarding their chemical composition and size distribution were selected as sorbates. HA, representing a more aromatic homogeneous fraction of DOM, was selected to represent interactions with (mostly aromatic) high molecular weight compounds and DOM from Suwannee River NOM (SRNOM) was employed as a natural, more aliphatic, lower molecular weight DOM. A compost extract DOM (CDOM) was chosen as a complex, environmentally representative DOM that contains a variety of undefined substances, polar macromolecules, and proteins. Graphite, carbon nanotubes and biochar, having distinct

structural properties, were used to compare the effects of different CM surface properties on sorption. These three different types of CMs represent (i) non-porous, mostly aromatic surfaces, (ii) strongly curved aromatic surfaces, and (iii) structurally heterogeneous carbonaceous surfaces with high porosity and a high number of functional groups, respectively. This study aimed to explain the discrepancies found between aromatic carbon content of a bulk DOM and its sorption affinity to CMs by separately analyzing the influence of DOM aromaticity and molecular weight as well as the CM surface properties on sorptive fractionation of structurally and compositionally complex different DOM.

## 2. Materials and methods

### 2.1 Materials

Commercial HA (technical grade, CAS number 1415-93-6) extracted from leonardite was purchased from Sigma Aldrich and SRNOM (RO isolate, 2R101N) from the International Humic Substances Society. CDOM was extracted from composted biosolids according to a protocol by Bhaduri *et al.*<sup>19</sup> DOM stock solutions were prepared by dissolving the dry material in ultrapure water (MQ, 18.2 M $\Omega$  cm, PURELAB Ultra, ELGA LabWater Global Operations), adjusted to pH 8.3 with 0.1 M NaOH to dissolve the material and re-adjusted regularly for 3 days while being agitated on a reciprocal shaker at 125 rpm. After 3 days the solution was adjusted to pH 7 with 0.1 M HCl, centrifuged ( $rcf = 1000 \times g$ ) for 30 minutes, and the supernatant then filtered through a sterile 0.22  $\mu\text{m}$  PES filter (Thermo Scientific, Nalgene, Rapid-Flow). HA was dialyzed (molecular weight cutoff 1 kDa) against MQ for 7 days and HA and CDOM was then purified with Chelex resin (complexing cation exchanger, Sigma-Aldrich, Chelex® 100 sodium form, dry mesh 50-100) to minimize possible effects of inorganic ions on the observed interactions.

Graphite (Sigma Aldrich, 99.99% carbon, CAS: 7782-42-5, <20  $\mu\text{m}$  powder) and single-walled carbon nanotubes (Sigma Aldrich,  $\geq 95\%$  carbon, CAS: 308068-56-6) were purchased from Sigma Aldrich and used as received. Single-walled carbon nanotubes were chosen as a well-defined and material with the minimum amount of surface functional groups that distinguishes itself from graphite mostly through its tubular geometry. This would allow a more direct comparison of effects that can be attributed to the sorbent geometry. Biochar (SWP700, UK Biochar Research Center, produced from soft wood pellets pyrolyzed at 700 °C) was crushed and sieved to obtain a size fraction of 64–250  $\mu\text{m}$ . To avoid measurement interference the leachable organic carbon fraction was removed by pre-leaching the biochar in MQ water (2 g L<sup>-1</sup>) for 24 hours, followed by wet sieving (64  $\mu\text{m}$ ).<sup>20</sup> The retained biochar was then oven-dried at 40 °C.

### 2.2 Sorbent characterization

The specific surface area and pore size distribution of the sorbents were derived from sorption isotherms of N<sub>2</sub> at 77 K after degassing overnight under a vacuum at 373.15 K, using a Quantachrome Nova 2000 Surface Area and Pore Size Analyzer,



following a protocol by Sigmund *et al.*<sup>21</sup> The total C, H, N and S content was measured using an elemental analyzer (Vario MACRO, Elementar), the ash content was determined by loss on ignition (750 °C, 4 hours), and the oxygen content was estimated by mass balance: O [wt%] = 100 – (C + H + N + S + ash content). The results are listed in Table S1.† Surface functional groups for all sorbents were determined by Fourier transform infrared (FT-IR) measurements (Fig. S1) as detailed in the ESI.†

### 2.3 Sorption experiments

Between 0.2 and 20 g L<sup>-1</sup> of sorbent was suspended in DOM solutions with 30 mg C L<sup>-1</sup> to achieve approximately 20% sorption of DOM. Samples were prepared in 50 mL vials with Teflon screw caps and placed on a reciprocating platform shaker at 125 rpm under exclusion of light. After an equilibration time of 7 days (chosen based on previously conducted kinetic studies<sup>10,22–24</sup>) the samples were centrifuged ( $rcf = 1000 \times g$ ) for 30 minutes and filtered (0.22 μm (ref. 17, 23 and 25–27)) for analysis of the DOM remaining in solution. Sample batches included duplicate samples and sorbent blanks, to avoid pH and temperature disturbance in our observations, all experiments were conducted at constant conditions (pH 7 at 274 K). The pH was monitored before and after the experiments: it remained constant at  $7.1 \pm 0.3$ . The amount of DOM in the supernatant was quantified after sorption to the CMs using a TOC analyzer (Shimadzu, TOC-L series), measuring non-purgeable organic carbon (NPOC). Samples containing biochar were corrected for blank values. Surface area normalized sorption coefficients ( $K_{SA}$ ) were calculated as  $(C_{sorbed}/\text{specific surface area})/C_{aqueous}$ .

The UV absorbance was measured using a UV/vis spectrophotometer (PerkinElmer, Lambda 35) with a 10 mm quartz cuvette.  $SUVA_{254}$  values were calculated by dividing the specific absorbance at 254 nm by the dissolved organic carbon (DOC) concentration ( $SUVA_{254} = 100 \times A_{254}/DOC$ ), which can be related to the aromaticity of the sample.<sup>4</sup> The ratios of specific UV absorbance at 250 nm to that at 365 nm ( $E_2/E_3$  ratios) being negatively correlated with aromaticity were calculated as an indicator of aromaticity.<sup>28,29</sup>

Fluorescence measurements were obtained using a spectrophotometer (Horiba FluoroMax 4) in a mirrored glass cuvette (1 cm path length) with a slit width of 3 nm and an integration time of 0.2 seconds. The fluorescence index (FI) was calculated as the ratio of the emission intensity at 470 nm to that at 520 nm, obtained at an excitation wavelength of 370 nm.<sup>30</sup> Measurements included peak C (ex. 340/em. 440 nm) and peak B (ex. 275/em. 305 nm), corresponding to the maximum fluorescence intensities of humic-like substances and tyrosine/protein-like substances, respectively.<sup>30</sup> The FI has an inverse correlation with both the degree of humification and the aromatic carbon content, and the C : B ratio describes the ratio of humic-like fluorophores to tyrosine-like fluorophores.<sup>29,31</sup> The C : B ratio was only used as a supporting indicator to predict aromaticity.

The molecular weight distribution of DOM before and after sorption was analyzed by size exclusion chromatography (SEC, XBridge® Protein BEH SEC 125 Å, 3.5 μm,

Waters). The column was used in a liquid chromatography system (Agilent Technologies 8800 Series) equipped with a UV/vis spectrophotometer (Agilent 1200 Series Diode Array and Multiple Wavelength Detector, detection at  $\lambda = 254$  nm and 365 nm) and a fluorescence detector (FLD, Agilent 1200 Series, excitation  $\lambda = 350$  nm, emission  $\lambda = 450$  nm). A flow rate of 0.4 mL min<sup>-1</sup> was used with a 25 mM sodium phosphate buffer (pH 6.7) as eluent and a sample injection volume of 30 μL. The samples were diluted in the eluent to avoid water peak interference. The column was calibrated with polystyrene sulfonate molecular weight standards (PSS, Polymer Standards Service GmbH) of 0.2, 1.1, 1.9, 3.6, 6.8 and 10.6 kDa. The column void volume was tested with polystyrene sulfonate (molecular weight 282 kDa) and the exclusion limit with acetone. Following elution, specific fractions (Fig. S2†) were collected using a fraction collector (Agilent 1200 Series). Signal data from both UV and fluorescence detectors were exported in milli absorbance units (mAU) and luminescence units (LU), respectively, and were analyzed using Origin® Graphing and Analysis software.

## 3. Results & discussion

### 3.1 The importance of DOM aromaticity for sorption depends on the sorbent properties

Graphite, carbon nanotubes and biochar all showed an overall preference for aromatic DOM fractions, as indicated by the spectroscopic measurements of CDOM, SRNOM and HA before and after sorption to these three sorbents (Fig. 1a–d). The  $SUVA_{254}$  values in the non-sorbed DOM fraction decreased slightly after sorption, indicating preferential sorption of the aromatic DOM fraction regardless of DOM type. While changes in the  $SUVA_{254}$  value were not always significant ( $p < 0.05$ ), the increase in  $E_2/E_3$  ratio following sorption to all CMs confirmed the preferential sorption of aromatic fractions, which is in line with previous observations.<sup>10,12,16,18,22</sup> The slight increase in the FI of DOM following sorption, accompanied by a decrease in the C : B ratio provided further confirmation that CMs had a general preference for aromatic DOM fractions. An exception was the FI of HA, which remained constant following sorption to carbon nanotubes. This may partially be explained as being a result of the high molecular weight of HA (Fig. 3) and the curved geometry of carbon nanotubes, as will be discussed in Section 3.2. In any case, HA is only one of the many constituents of heterogeneous natural DOM. The fact that the FI of both SRNOM and CDOM indicated a fractionation after sorption emphasizes the shortcomings of using HA as a DOM surrogate when investigating interactions in natural environments. Since HA represents a rather defined DOM fraction and only occupies specific types of sorption sites, it cannot reflect the full range of interactions that occur between DOM and CMs. Thus, HA may not respond in the same way as more complex DOM to changes in the factors that affect sorption.

DOM–CM interactions are mostly governed by hydrophobic effects and  $\pi$ – $\pi$  EDA interactions between aromatic carbon structures of the sorbent and the sorbate.<sup>32</sup> Interactions between graphite and the most aromatic DOM fractions are



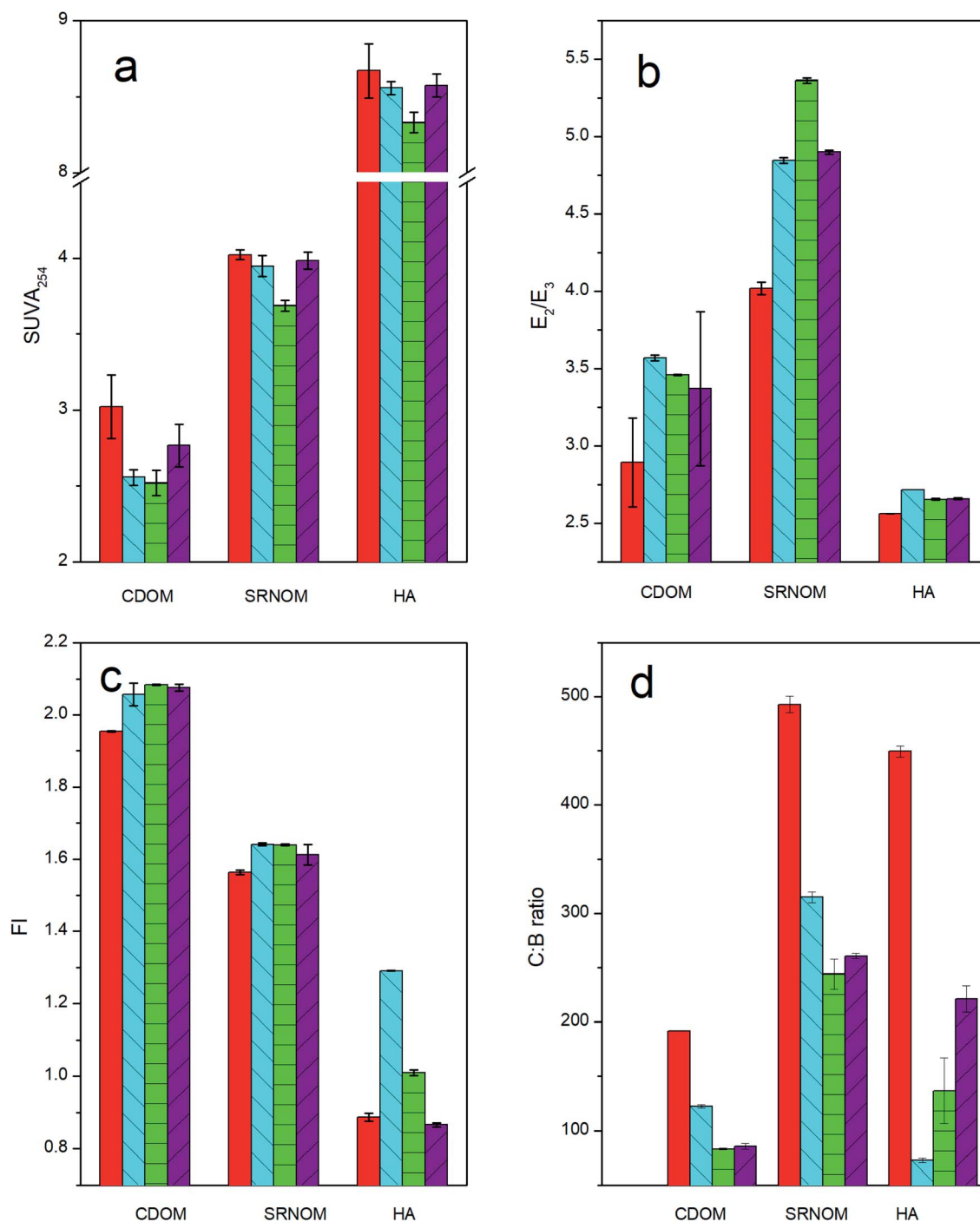


Fig. 1 Bar charts of (a) SUVA<sub>254</sub> values, (b) E<sub>2</sub>/E<sub>3</sub> ratios, (c) FI values, and (d) peak C : B ratios for CDOM, SRNOM, and HA prior to sorption (— red empty bars), and after sorption to biochar (— blue bars (//)), graphite (— green bars (==)), and carbon nanotubes (— purple bars (//)), showing an overall preference by CMs for aromatic DOM fractions. Error bars represent the standard deviation from triplicate measurements.

therefore strongly favored. The formation of H-bonds plays a minor role due to the absence of functional groups on the surface of graphite and carbon nanotubes (carbon purity is >99.99% and >95%, respectively; Table S1†), suggesting that DOM sorption to CMs occur mainly through  $\pi$ - $\pi$  EDA interactions.<sup>32</sup> This may explain why graphite in particular showed a strong preference for the aromatic fraction, as shown by the markedly reduced SUVA<sub>254</sub> values (Fig. 1a).

DOM with higher aromaticity was often found to result in a higher distribution coefficient ( $K_D$ ) for sorption to carbon nanotubes, graphite, or activated carbon.<sup>9,10,14,17</sup> However, Zhang *et al.* (2015) found that the  $K_D$  for sorption of HA to carbon nanotubes decreased systematically with increasing molecular weight and aromaticity.<sup>33</sup> Recently Engel and Chefetz (2019) presented a linear correlation between the percentage of aromatic carbon and the extent of HA or FA sorption to carbon nanotubes.<sup>5</sup> However, this





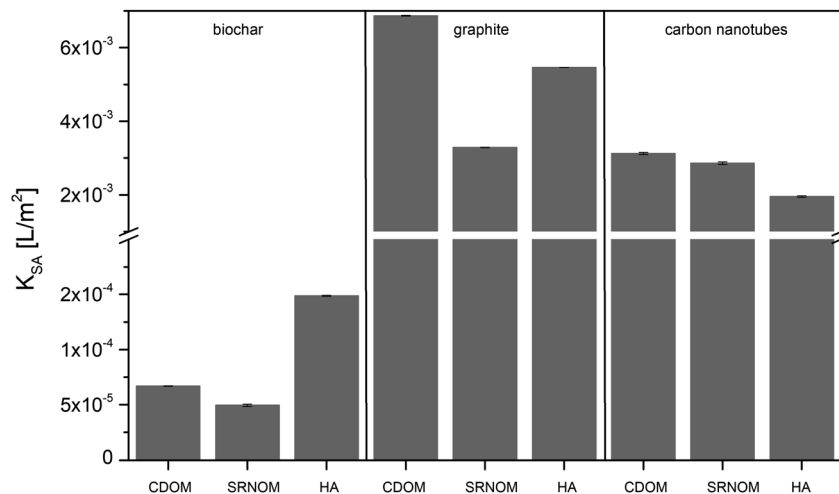


Fig. 2 Sorption coefficients ( $K_{SA}$ ) of three types of DOM (CDOM, SRNOM, and HA) to biochar, graphite, and carbon nanotubes. Error bars represent the standard deviation from triplicate measurements.

correlation could not be confirmed when extending the comparison across multiple studies and a range of different types of DOM, rather than just FA and HA. The lack of any linear correlation between aromatic carbon content and the adsorption coefficient indicates that there are additional factors that need to be considered. Our findings show that the properties of the sorbent can affect the importance of aromaticity for sorption (Fig. 2).

$K_{SA}$  values for graphite and carbon nanotubes were considerably greater than that for biochar. This can be explained by the negative charges on the biochar surface that can cause electrostatic repulsion of the negatively charged DOM, reducing the  $K_{SA}$  considerably.<sup>34</sup> Furthermore, CMs show a preference for aromatic DOM fractions, which can form  $\pi$ - $\pi$  EDA interactions with the aromatic surfaces of the CMs.<sup>34</sup> Graphite and carbon nanotube surfaces consist of aromatic sheets of carbon, whereas biochar surfaces can contain plenty of oxygen-containing functional groups among the aromatic surface patches.<sup>35</sup> These highly condensed aromatic patches are usually smaller than 5 nm as demonstrated by high-resolution transmission electron microscopy of high temperature biochar surfaces.<sup>36</sup> The highest  $K_{SA}$  values would therefore be expected for the most aromatic bulk DOM sorbing to graphite or carbon nanotubes. Fig. 1 shows that HA is the most aromatic bulk DOM in our set, but it was nevertheless not the most strongly sorbed by either graphite or carbon nanotubes. Although biochar mostly showed a less marked preference than graphite for the aromatic DOM fraction (Fig. 1) it sorbed HA, the overall most aromatic bulk DOM, more strongly than it sorbed SRNOM or CDOM. This supports the hypothesis that DOM aromaticity is an important factor affecting DOM sorption to all types of CMs (Fig. 1), but that on its own it is unable to account for all differences in DOM sorption, as discussed in the following sections.

### 3.2 DOM fractionation is controlled by the interplay between sorbate molecular weight and sorbent geometry

Although DOM aromaticity generally correlates with molecular weight, this does not necessarily apply for all DOM types.<sup>16</sup> Since

both factors can exert different influences on sorption, in a first step they have been considered separately in this study. Firstly, to investigate the influence of molecular weight on sorption, size exclusion chromatograms of the three DOMs were measured before and after sorption to CMs (Fig. 3a and S3†). Our data show that graphite strongly sorbed the fraction with molecular weights between 1 kDa and 3 kDa, biochar was less selective and sorbed all fractions with molecular weights >1 kDa, and carbon nanotubes mainly sorbed those fractions with molecular weights <1 kDa. The increase in high molecular weight DOM during HA sorption by biochar is most likely due to aggregation of smaller HA molecules due to the release of calcium from biochar samples.<sup>37</sup> Although each sorbent preferentially sorbed a different molecular weight fraction, the aromatic DOM fractions were preferred by all sorbents, as shown in Section 3.1. To understand the combined influence that both factors have on sorption, we investigated the aromaticity of each of the preferentially sorbed fractions separately (Fig. S2 and S4 and Table S2†).

The  $SUVA_{254}$  values decreased together with molecular weight, thus linking aromaticity with molecular weight – as has been previously reported for other types of DOM.<sup>28,38</sup> This appears to contradict the observation that carbon nanotubes preferentially sorbed the aromatic fraction (as supported by the spectroscopic aromaticity indicators shown in Fig. 1) and yet showed preferential sorption of the smaller and relatively less aromatic fractions with molecular weights of <1 kDa (Fig. 3a). A possible explanation can be derived from SEC measurements with simultaneous detection at 250 nm and 365 nm, which yielded the  $E_2/E_3$  ratio of each molecular weight fraction before and after sorption (Fig. 3b). As the  $E_2/E_3$  ratio is inversely correlated with aromaticity the graphs show the aromaticity of the original DOM and the DOM after sorption for each molecular weight.

The  $E_2/E_3$  ratio for the smaller molecular weight DOM fraction that was preferentially sorbed by carbon nanotubes was considerably greater than that for the non-sorbed DOM



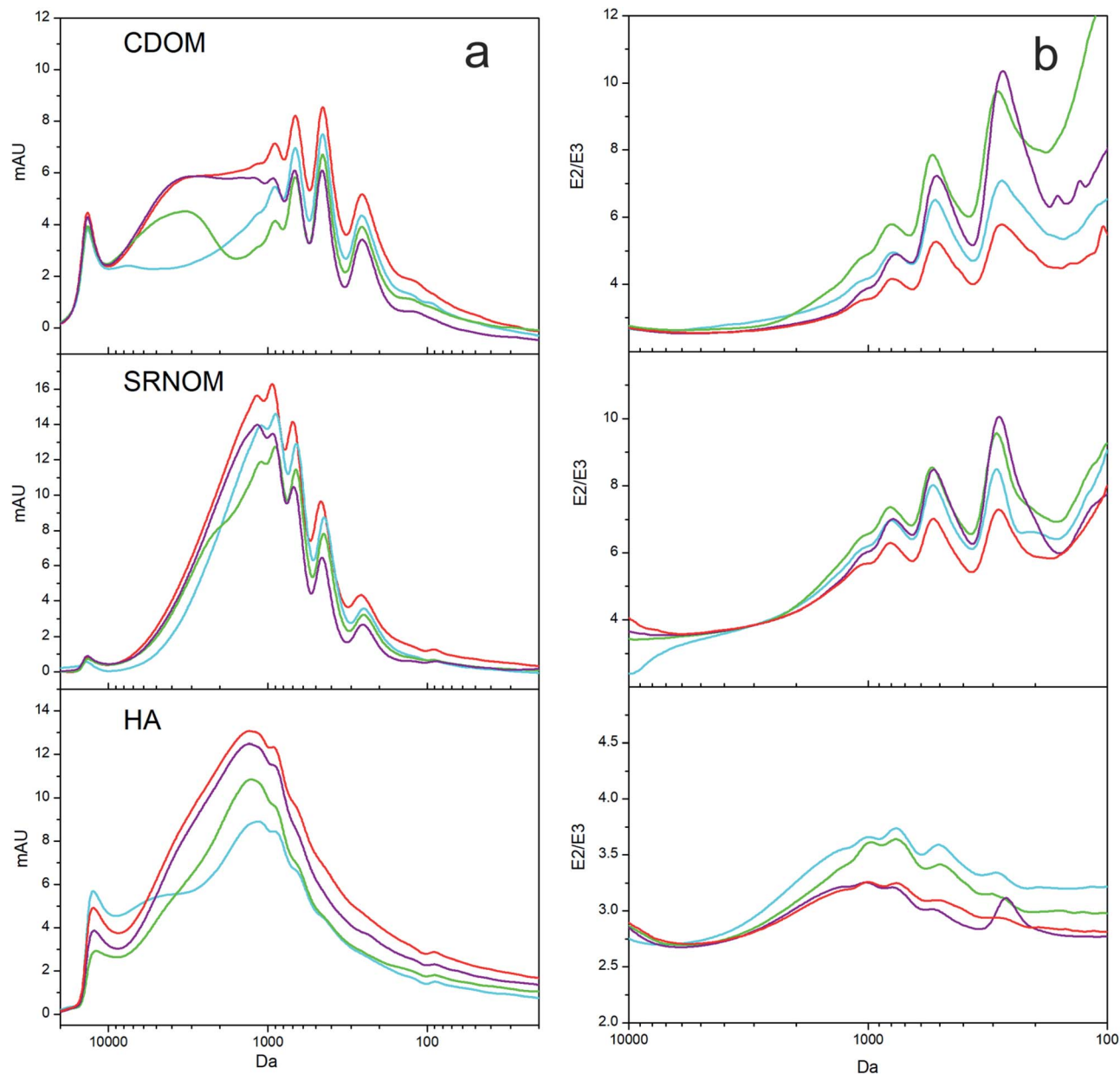


Fig. 3 SEC chromatograms of CDOM, SRNOM and HA, prior to sorption (— red line), and following sorption to biochar (— blue line), graphite (— green line), and carbon nanotubes (— purple line) (a) detected at 254 nm, showing the preferential sorption of specific DOM molecular weight fractions by each sorbent, (b) showing an increase in  $E_2/E_3$  ratios especially throughout the lower molecular weight of all DOM types following sorption by each sorbent, demonstrating preferential sorption of aromatic DOM fraction within each molecular weight fraction.

(Fig. 3b), indicating preferential sorption of aromatic compounds within each molecular weight fraction. Although the spectroscopic measurements (Fig. S4†) indicate that the smaller molecular weight fractions were less aromatic overall, Fig. 3b illustrates that there were aromatic compounds present within the smaller molecular weight fractions that were preferentially sorbed. This is therefore consistent with an overall preference for the aromatic fraction in bulk measurements (Fig. 1). All three sorbents showed a stronger fractionation in the lower molecular weight range (Fig. 3b). Single-walled carbon nanotubes only sorbed these lower molecular weight compounds and accordingly only fractionated these. Biochar

and graphite, however, especially sorbed the higher molecular weight compounds but showed a stronger fractionation in the lower molecular weight range. This indicates that the lower molecular weight compounds are chemically more heterogeneous; while the high molecular weight compounds (2.5–1 kDa) are mostly aromatic, the smaller fractions contain both aliphatic and aromatic compounds resulting in a stronger chemical fractionation. The highest molecular weight fraction (>2.5 kDa) contains high amounts of tyrosine- and protein-like compounds which is shown by the fluorescence measurements (Fig. S5†) but possibly not detected by the  $E_2/E_3$  ratio measurements (Fig. 3b). Thus, the highest molecular weight



fraction could be equally fractionated as the smaller one. Sorbent surface properties and geometry can explain why higher molecular weight DOM fractions are sorbed less by carbon nanotubes (Fig. 2) despite being more aromatic. The carbon nanotube pore size distribution (Fig. S6†) extends over a large range of mesopores with pore widths between 3 and 15 nm. However, the use of pore size distributions for carbon nanotubes has to be interpreted with caution as the dry aggregated powder may exhibit different pores than the actual dispersed carbon nanotubes in water. Sorbed DOM disperses and stabilizes carbon nanotubes in solution and may limit DOM sorption in the interstitial spaces between carbon nanotube bundles.<sup>39,40</sup> The inner pores of carbon nanotubes are too small for the diffusion of DOM molecules and it has been argued that possible sorption mostly occurs on the cylindrical surface of the outermost carbon nanotubes.<sup>17,18,41</sup> Pore exclusion effects can hardly explain the selectivity of carbon nanotubes for certain molecular weight fractions; most studies to date found preferential adsorption of higher molecular weight fractions of DOM by carbon nanotubes since that this is the most aromatic fraction.<sup>10,14,17,18</sup> Although the sorption of some of the DOM fractions may occur in the grooves of carbon nanotube aggregates,<sup>42</sup> it does not explain the exclusion of the higher molecular weight fractions that are overall more aromatic than the lower molecular weight fractions. Carbon nanotubes preferentially sorbed aromatic compounds even within the small MW fractions (Fig. 3b), which demonstrates the influence of the sorbent geometry. Aromatic structures are relatively rigid, with low rotational degrees of freedom; they are consequently not able to adjust their conformation to the highly curved surfaces of carbon nanotube with small diameters and thereby increase the contact area.<sup>30,33</sup> This restricts sorption to only the smaller aromatic compounds, which maintain the face-to-face orientation allowing  $\pi$ - $\pi$  EDA interactions to take place<sup>32</sup> and is supported by the previous finding that HA sorption to carbon nanotubes decreases as their outer diameter decreases<sup>13</sup> and as the molecular weight of the HA increases.<sup>33</sup>

It was previously suggested that aliphatic compounds have a high affinity to carbon nanotubes due to their rotational degrees of freedom resulting in an improved structural compatibility than rigid aromatic compounds.<sup>33</sup> However, this study showed that the sorption of smaller molecular weight DOM by carbon nanotubes does not correlate with a preference for aliphatic and less aromatic compounds. Aromatic compounds are, in fact, preferentially sorbed despite being less abundant in the small molecular weight fractions. This shows that aromaticity is a key factor determining adsorption to carbonaceous materials when considering pure and defined sorbent structures. For more heterogeneous sorbent surfaces as found in the natural environment polar and aliphatic moieties can play a considerable role for sorption.<sup>43</sup>

### 3.3 Sorbent heterogeneity decreases selectivity for aromatic fractions

Of the sorbents investigated, graphite showed the strongest preference for the aromatic DOM fraction (Fig. 1). Accordingly,

the molecular weight fraction between 1 kDa and 3 kDa, which was the most aromatic fraction according to the SUVA<sub>254</sub> value and the C : B ratio (Fig. S4†), was the fraction most efficiently sorbed by graphite (Fig. 3a). Aromatic molecules can maximize their contact areas on graphene surfaces because of their planar nature, in contrast to the strongly curved surfaces of carbon nanotubes.<sup>44</sup> Interactions between aromatic high molecular weight fractions and the planar aromatic graphite surfaces are therefore favored.

Graphite sorbed the highest molecular weight fraction (>3 kDa) considerably less effectively than the fraction with molecular weights between 1 and 3 kDa (Fig. 3a) due to differences in composition between the two fractions. Although earlier observations that aromaticity generally decreases with molecular weight were confirmed, the C : B ratio of the highest molecular weight fraction was lower than that of the second-highest fraction (Fig. S4†). The comparably more pronounced peak B indicates the presence of protein-like or tyrosine-like compounds.<sup>30</sup> Furthermore, SEC chromatograms indicated the presence of protein-like and tryptophan-like compounds in the highest molecular weight fraction of CDOM (Fig. S5†).<sup>30</sup> This structurally more heterogeneous fraction sorbs to CM surfaces through different mechanisms than the more aromatic hydrophobic fractions do.<sup>12</sup> Graphite has hardly any surface functional groups and preferably sorbs the aromatic DOM fraction through hydrophobic and  $\pi$ - $\pi$  EDA interactions on its planar aromatic surface. Biochar, on the other hand, contains functional groups on its otherwise carbonized and aromatic surface. Previous research on SWP700 biochar has identified surface functional groups by FT-IR,<sup>45,46</sup> Boehm titration,<sup>47</sup> and X-ray photoelectron spectroscopy.<sup>48</sup> FT-IR measurements (Fig. S1†) indicate the presence of functional groups such as hydroxyl groups that can exert a different sorption behavior than the graphite or carbon nanotube surfaces: next to  $\pi$ - $\pi$  EDA interactions and hydrophobic effects, which contribute strongly to sorption to the aromatic surface patches of biochar, electrostatic interactions and the formation of H-bonds between oxygen-containing functional groups of biochar and polar groups of DOM can occur. Biochar therefore sorbed the highest molecular weight fraction just as strongly as the second-highest molecular weight fraction, despite their different chemical characteristics. In contrast, graphite preferentially sorbed the second-highest molecular weight fraction, which did not contain as much polar less aromatic carbon as the highest molecular weight fraction. Furthermore, polar interactions were shown to strongly contribute to the sorption of HA to graphene oxides.<sup>49</sup> The relative contribution of each type of interaction is dependent on the abundance of surface functional groups.<sup>10,25</sup> Low temperature produced biochars have a lower aromaticity and higher number of functional groups and better adsorb polar DOM compared to the high temperature SWP700 used in this study.<sup>25</sup>

Previous studies explained sorption of distinct molecular weight fractions by pore sieving, *i.e.*, large organic molecules and high molecular weight DOM molecular weight are excluded from micro- and mesopores.<sup>14,15</sup> The biochar pore size distribution (Fig. S6†) shows that biochar has a large mesopore



volume between 1.8 and 2 nm. Measurements of the same biochar material by Sigmund *et al.* (2017) show that a large proportion of pores are in the micropore range<sup>21</sup> which are likely inaccessible for most DOM molecules.<sup>24,50</sup> Although sorption of the smallest DOM fractions in the range of the measured lower mesopores and reported micropores may have occurred through pore filling, pore sieving effects do not explain the sorption of the fraction >1 kDa.

## 4 Conclusion

The ubiquitous input of highly aromatic CMs to surface waters can influence the composition of the DOM, which can in turn affect the fate of both DOM and CMs. By individually investigating sorptive fractionation of three compositionally different DOM types we could demonstrate how DOM–CM interactions are influenced by a variety of factors including aromaticity, molecular weight, sorbent functionality, and sorbent geometry. Most importantly, these factors were interdependent and could not be considered independently. It is therefore possible for a rather aromatic DOM fraction to not be sorbed because of other factors such as the sorbate molecular weight or sorbent geometry not being favorable for sorption. This may have led to discrepancies between the results of previous investigations and needs to be considered in any future research.

HA is often used as a surrogate for natural DOM and its influence on processes occurring under natural conditions, even though it only represents a discrete fraction of the highly heterogeneous DOM. Our investigations have shown that this influences the way it interacts with CMs, so that the choice of DOM can have a strong influence on the outcome of any experiment, especially when ternary interactions are analyzed. It is therefore critically important in any future research to consider carefully the choice of DOM to be used as environmentally representative DOM.

## Conflicts of interest

There are no conflicts to declare.

## Acknowledgements

This study was funded by the Austrian Science Fund (FWF), project number P 27689-N28. We thank Bhaskar Bhaduri for kindly providing DOM from compost extracts.

## References

- J. J. Cole, Y. T. Prairie, N. F. Caraco, W. H. McDowell, L. J. Tranvik, R. G. Striegl, C. M. Duarte, P. Kortelainen, J. A. Downing, J. J. Middelburg and J. Melack, Plumbing the global carbon cycle: integrating inland waters into the terrestrial carbon budget, *Ecosystems*, 2007, **10**, 171–184, DOI: 10.1007/s10021-006-9013-8.
- H. Xu and L. Guo, Molecular size-dependent abundance and composition of dissolved organic matter in river, lake and sea waters, *Water Res.*, 2017, **117**, 115–126, DOI: 10.1016/j.watres.2017.04.006.
- T. Polubesova and B. Chefetz, DOM-affected transformation of contaminants on mineral surfaces: a review, *Crit. Rev. Environ. Sci. Technol.*, 2014, **44**, 223–254, DOI: 10.1080/10643389.2012.710455.
- J. A. Leenheer and J.-P. Croué, Characterizing Dissolved Aquatic Organic Matter, *Environ. Sci. Technol.*, 2003, **37**, 18A–26A, DOI: 10.1021/es032333c.
- M. Engel and B. Chefetz, The missing link between carbon nanotubes, dissolved organic matter and organic pollutants, *Adv. Colloid Interface Sci.*, 2019, **271**, 101993, DOI: 10.1016/j.cis.2019.101993.
- W. Yang, Y. Wang, J. Shang, K. Liu, P. Sharma, J. Liu and B. Li, Antagonistic effect of humic acid and naphthalene on biochar colloid transport in saturated porous media, *Chemosphere*, 2017, **189**, 556–564, DOI: 10.1016/j.chemosphere.2017.09.060.
- G. Sigmund, C. Jiang, T. Hofmann and W. Chen, Environmental transformation of natural and engineered carbon nanoparticles and implications for the fate of organic contaminants, *Environ. Sci.: Nano*, 2018, **5**, 2500–2518, DOI: 10.1039/c8en00676h.
- M. R. Wiesner, G. V. Lowry, P. Alvarez, D. Dionysiou and P. Biswas, Assessing the Risks of Manufactured Nanomaterials, *Environ. Sci. Technol.*, 2006, **40**, 4336–4345.
- M. Ateia, O. G. Apul, Y. Shimizu, A. Muflihah, C. Yoshimura and T. Karanfil, Elucidating Adsorptive Fractions of Natural Organic Matter on Carbon Nanotubes, *Environ. Sci. Technol.*, 2017, **51**, 7101–7110, DOI: 10.1021/acs.est.7b01279.
- N. Cai, D. Peak and P. Larese-Casanova, Factors influencing natural organic matter sorption onto commercial graphene oxides, *Chem. Eng. J.*, 2015, **273**, 568–579, DOI: 10.1016/j.cej.2015.03.108.
- K. Yang, Y. Jiang, J. Yang and D. Lin, Correlations and adsorption mechanisms of aromatic compounds on biochars produced from various biomass at 700 °C, *Environ. Pollut.*, 2018, **233**, 64–70, DOI: 10.1016/j.envpol.2017.10.035.
- M. B. Ahmed, M. A. H. Johir, C. Khoureshed, J. L. Zhou, H. H. Ngo, D. L. Nghiem, M. Moni and L. Sun, Sorptive removal of dissolved organic matter in biologically-treated effluent by functionalized biochar and carbon nanotubes: importance of sorbent functionality, *Bioresour. Technol.*, 2018, **269**, 9–17, DOI: 10.1016/j.biortech.2018.08.046.
- X. Wang, L. Shu, Y. Wang, B. Xu, Y. Bai, S. Tao and B. Xing, Sorption of Peat Humic Acids to Multi-Walled Carbon Nanotubes, *Environ. Sci. Technol.*, 2011, **45**, 9276–9283, DOI: 10.1021/es202258q.
- Y. Shimizu, M. Ateia and C. Yoshimura, Natural organic matter undergoes different molecular sieving by adsorption on activated carbon and carbon nanotubes, *Chemosphere*, 2018, **203**, 345–352, DOI: 10.1016/j.chemosphere.2018.03.197.
- C. Lattao, X. Cao, J. Mao, K. Schmidt-Rohr and J. J. Pignatello, Influence of Molecular Structure and Adsorbent Properties on Sorption of Organic Compounds





- to a Temperature Series of Wood Chars, *Environ. Sci. Technol.*, 2014, **48**, 4790–4798, DOI: 10.1021/es405096q.
- 16 K. K. Shimabuku, A. M. Kennedy, R. E. Mulhern and R. S. Summers, Evaluating Activated Carbon Adsorption of Dissolved Organic Matter and Micropollutants Using Fluorescence Spectroscopy, *Environ. Sci. Technol.*, 2017, **51**, 2676–2684, DOI: 10.1021/acs.est.6b04911.
- 17 H. Hyung and J.-H. Kim, Natural Organic Matter (NOM) Adsorption to Multi-Walled Carbon Nanotubes: Effect of NOM Characteristics and Water Quality Parameters, *Environ. Sci. Technol.*, 2008, **42**, 4416–4421, DOI: 10.1021/es702916h.
- 18 K. Yang and B. Xing, Adsorption of fulvic acid by carbon nanotubes from water, *Environ. Pollut.*, 2009, **157**, 1095–1100, DOI: 10.1016/j.envpol.2008.11.007.
- 19 B. Bhaduri, T. Polubesova and B. Chefetz, Interactions of organic dye with Ag- and Ce-nano-assemblies: influence of dissolved organic matter, *Colloids Surf., A*, 2019, **577**, 683–694, DOI: 10.1016/j.colsurfa.2019.06.026.
- 20 B. Wang, W. Zhang, H. Li, H. Fu, X. Qu and D. Zhu, Micropore clogging by leachable pyrogenic organic carbon: a new perspective on sorption irreversibility and kinetics of hydrophobic organic contaminants to black carbon, *Environ. Pollut.*, 2017, **220**, 1349–1358, DOI: 10.1016/j.envpol.2016.10.100.
- 21 G. Sigmund, T. Hüffer, T. Hofmann and M. Kah, Biochar total surface area and total pore volume determined by N<sub>2</sub> and CO<sub>2</sub> physisorption are strongly influenced by degassing temperature, *Sci. Total Environ.*, 2017, **580**, 770–775, DOI: 10.1016/j.scitotenv.2016.12.023.
- 22 M. Engel and B. Chefetz, Adsorptive fractionation of dissolved organic matter (DOM) by carbon nanotubes, *Environ. Pollut.*, 2015, **197**, 287–294, DOI: 10.1016/j.envpol.2014.11.020.
- 23 B. Smith, J. Yang, J. L. Bitter, W. P. Ball and D. H. Fairbrother, Influence of Surface Oxygen on the Interactions of Carbon Nanotubes with Natural Organic Matter, *Environ. Sci. Technol.*, 2012, **46**, 12839–12847, DOI: 10.1021/es303157r.
- 24 G. Kasozi, A. Zimmermann, P. Nkedi-Kizza and B. Gao, Catechol and Humic Acid Sorption onto a Range of Laboratory-Produced Black Carbons (Biochars), *Environ. Sci. Technol.*, 2010, **44**, 6189–6195, DOI: 10.1021/es1014423.
- 25 F. Lian, B. Sun, X. Chen, L. Zhu, Z. Liu and B. Xing, Effect of humic acid (HA) on sulfonamide sorption by biochars, *Environ. Pollut.*, 2015, **204**, 306–312, DOI: 10.1016/j.envpol.2015.05.030.
- 26 Q. Zhou, S. Ouyang, Z. Ao, J. Sun, G. Liu and X. Hu, Integrating Biolayer Interferometry, Atomic Force Microscopy and Density Functional Theory Calculation Studies on the Affinity between Humic Acid Fractions and Graphene Oxide, *Environ. Sci. Technol.*, 2019, **53**, 3773–3781, DOI: 10.1021/acs.est.8b05232.
- 27 X. Zhou, L. Shu, H. Zhao, X. Guo, X. Wang, S. Tao and B. Xing, Suspending Multi-Walled Carbon Nanotubes by Humic Acids from a Peat Soil, *Environ. Sci. Technol.*, 2012, **46**, 3891–3897, DOI: 10.1021/es204657k.
- 28 J. Peuravuori and K. Pihlaja, Molecular size distribution and spectroscopic properties of aquatic humic substances, *Anal. Chim. Acta*, 1997, **337**, 133–149, DOI: 10.1016/S0003-2670(96)00412-6.
- 29 M. Ateia, J. Ran, M. Fujii and C. Yoshimura, The relationship between molecular composition and fluorescence properties of humic substances, *Int. J. Environ. Sci. Technol.*, 2017, **14**, 867–880, DOI: 10.1007/s13762-016-1214-x.
- 30 G. R. Aiken, in *Aquatic organic matter fluorescence*, ed. P. G. Coble, J. Lead, A. Baker, D. M. Reynolds and R. G. M. Spencer, Cambridge University Press, New York, 2014, pp. 35–74, DOI: 10.1017/CBO9781139045452.005.
- 31 P. G. Coble, J. Lead, A. Baker, D. M. Reynolds and R. G. M. Spencer, *Aquatic organic matter fluorescence*, 2014.
- 32 D. Zhu and J. J. Pignatello, Characterization of aromatic compound sorptive interactions with black carbon (charcoal) assisted by graphite as a model, *Environ. Sci. Technol.*, 2005, **39**, 2033–2041, DOI: 10.1021/es0491376.
- 33 D. Zhang, B. Pan, R. L. Cook and B. Xing, Multi-walled carbon nanotube dispersion by the adsorbed humic acids with different chemical structures, *Environ. Pollut.*, 2015, **196**, 292–299, DOI: 10.1016/j.envpol.2014.10.020.
- 34 G. Newcombe and M. Drikas, Adsorption of NOM onto Activated Carbon: Electrostatic and Non-electrostatic Effects, *Carbon*, 1997, **35**, 1239–1250.
- 35 J. Lehmann and S. Joseph, in *Biochar for environmental management*, Earthscan, London, 1st edn, 2009.
- 36 X. Xiao and B. Chen, A Direct Observation of the Fine Aromatic Clusters and Molecular Structures of Biochars, *Environ. Sci. Technol.*, 2017, **51**, 5473–5482, DOI: 10.1021/acs.est.6b06300.
- 37 P. M. Melia, R. Busquets, P. S. Hooda, A. B. Cundy and S. P. Sohi, Driving forces and barriers in the removal of phosphorus from water using crop residue, wood and sewage sludge derived biochars, *Sci. Total Environ.*, 2019, **675**, 623–631, DOI: 10.1016/j.scitotenv.2019.04.232.
- 38 M. Shen, X. Hai, Y. Shang, C. Zheng, P. Li, Y. Li, W. Jin, D. Li, Y. Li, J. Zhao, H. Lei, H. Xiao, Y. Li, G. Yan, Z. Cao and Q. Bu, Insights into aggregation and transport of graphene oxide in aqueous and saturated porous media: complex effects of cations with different molecular weight fractionated natural organic matter, *Sci. Total Environ.*, 2019, **656**, 843–851, DOI: 10.1016/j.scitotenv.2018.11.387.
- 39 H. Hyung, J. D. Fortner, J. B. Hughes and J. H. Kim, Natural organic matter stabilizes carbon nanotubes in the aqueous phase, *Environ. Sci. Technol.*, 2007, **41**, 179–184, DOI: 10.1021/es061817g.
- 40 X. Zhang, M. Kah, M. T. O. Jonker and T. Hofmann, Dispersion state and humic acids concentration-dependent sorption of pyrene to carbon nanotubes, *Environ. Sci. Technol.*, 2012, **46**, 7166–7173, DOI: 10.1021/es300645m.
- 41 D. Lin, T. Li, K. Yang and F. Wu, The relationship between humic acid (HA) adsorption on and stabilizing multiwalled carbon nanotubes (MWNTs) in water: effects of HA, MWNT and solution properties, *J. Hazard. Mater.*, 2012, **241–242**, 404–410, DOI: 10.1016/j.jhazmat.2012.09.060.



- 42 S. Agnihotri, M. Rostam-Abadi and M. J. Rood, Temporal changes in nitrogen adsorption properties of single-walled carbon nanotubes, *Carbon*, 2004, **42**, 2699–2710, DOI: 10.1016/j.carbon.2004.06.016.
- 43 B. Chefetz and B. Xing, Relative role of aliphatic and aromatic moieties as sorption domains for organic compounds: a review, *Environ. Sci. Technol.*, 2009, **43**, 1680–1688, DOI: 10.1021/es803149u.
- 44 K. Yang and B. Xing, Adsorption of organic compounds by carbon nanomaterials in aqueous phase: Polanyi theory and its application, *Chem. Rev.*, 2010, **110**, 5989–6008, DOI: 10.1021/cr100059s.
- 45 N. Alozie, N. Heaney and C. Lin, Biochar immobilizes soil-borne arsenic but not cationic metals in the presence of low-molecular-weight organic acids, *Sci. Total Environ.*, 2018, **630**, 1188–1194, DOI: 10.1016/j.scitotenv.2018.02.319.
- 46 N. Heaney, M. Mamman, H. Tahir, A. Al-Gharib and C. Lin, Effects of softwood biochar on the status of nitrogen species and elements of potential toxicity in soils, *Ecotoxicol. Environ. Saf.*, 2018, **166**, 383–389, DOI: 10.1016/j.ecoenv.2018.09.112.
- 47 P. M. Melia, R. Busquets, P. S. Hooda, A. B. Cundy and S. P. Sohi, Driving forces and barriers in the removal of phosphorus from water using crop residue, wood and sewage sludge derived biochars, *Sci. Total Environ.*, 2019, **675**, 623–631, DOI: 10.1016/j.scitotenv.2019.04.232.
- 48 D. Ziegler, P. Palmero, M. Giorcelli, A. Tagliaferro and J. M. Tulliani, Biochars as innovative humidity sensing materials, *Chemosensors*, 2017, **5**, 1–16, DOI: 10.3390/chemosensors5040035.
- 49 S. Yang, L. Li, Z. Pei, C. Li, X. Shan, B. Wen, S. Zhang, L. Zheng, J. Zhang, Y. Xie and R. Huang, Effects of humic acid on copper adsorption onto few-layer reduced graphene oxide and few-layer graphene oxide, *Carbon*, 2014, **75**, 227–235, DOI: 10.1016/j.carbon.2014.03.057.
- 50 R. S. Summers and P. V. Roberts, Activated Carbon Adsorption of Humic Substances II. Size Exclusion and Electrostatic Interactions, *J. Colloid Interface Sci.*, 1988, **122**, 382–397, DOI: 10.1016/0021-9797(88)90373-6.

